Heliyon 9 (2023) e12922

Contents lists available at ScienceDirect

Heliyon

journal homepage: www.cell.com/heliyon

Research article

Characteristics of SI engine fueled with BE50-Isooctane blends with different ignition timings

Suyatno [a], Helen Riupassa [a], Susi Marianingsih [b], Hendry Y. Nanlohy [a,*]

[a] Department of Mechanical Engineering, Jayapura University of Science and Technology, 99351, Indonesia
[b] Faculty of Computer Science and Management, Jayapura University of Science and Technology, 99351, Indonesia

ARTICLE INFO

Keywords:
Bioethanol
Isooctane
Molecular properties
Ignition timing
Engine characteristic
Spark ignition

ABSTRACT

The effect of various ignition timing on spark ignition (SI) engines with bioethanol-isooctane mixtures has been widely studied. In the present studies, we used three different ignition angle positions, namely 9°, 12°, and 15° BTDC to increase the combustion pressure in the combustion chamber. In addition to macroscopic observations through engine performance, observations are also carried out from a molecular perspective, i.e.; atomic, bond, and bond angle properties of bioethanol-isooctane fuel. The result shows that more atoms of the isooctane carbon chain are non-rotatable (23 atomic bonds) than the 8 bonds of the bioethanol carbon chain. Furthermore, isooctane also has a wider bond angle (around 121.1745°) than the bond angle of ethanol (around 110.0476°). The unique properties of the atoms in the carbon chains of these two fuels have a direct impact on engine performance. The results show that the viscosity of bioethanol is lower when compared to isooctane, which indicates that the bioethanol molecules are more reactive and flammable. The result also found that at an ignition angle of 12° the BE50 engine has the best performance. Moreover, the test results also show that bioethanol produces clean combustion as evidenced by the lowest CO and HC gas emissions.

1. Introduction

With the dwindling resources of crude oil and the increasing consumption of fuel in the transportation, industrial, and household sectors, as well as the increase in the global population, have resulted in an energy crisis [1-3]. This situation emphasizes the crucial solution for renewable fuels [4]. Bioethanol is one type of renewable fuel that can be a solution to overcome the fuel energy crisis because it can be applied to spark-ignition (SI) engines [5-7]. Furthermore, because the composition of the ethanol compound (see Table 1) makes it more soluble and oxygenated in isooctane [8], and because of the heat of vaporization, and low vapor pressure, bioethanol can be converted into a renewable fuel [9–11]. On the other hand, when compared to biodiesel [12], bioethanol has lower greenhouse gas emissions and production costs and has a more profitable future evolution; thus, bioethanol and its mixtures (gasoline, isooctane) have great potential to be used as renewable fuels, especially in SI engines and in modern vehicles [13-16]. In addition, a recent studies on the effect of a mixture of ethanol and isooctane on laminar burning characteristics [17–19], octane reaction on the methyl *tert*-butyl ether (MTBE) with gasoline [20]. Furthermore, application research on the effect of the use of ethanol and isooctane against flame speed [21], dynamic spray [22], macroscopic spray characteristics under flash boiling conditions [23,24], NOx emissions [25,26], particulate matter [27], and their impact on fuel efficiency have also been applied to the SI engine, and the results show that

* Corresponding author.
E-mail address: hynanlohy@gmail.com (H.Y. Nanlohy).

https://doi.org/10.1016/j.heliyon.2023.e12922
Received 8 September 2022; Received in revised form 7 January 2023; Accepted 9 January 2023
Available online 12 January 2023

there is a significant performance improvement [28-30].

However, previous research was carried out about bioethanol by modifying the ignition degree with a usual standard on the spark ignition engine [31,32]. These studies stated that the burning rate increased for all variaous blended of the bioethanol–isooctane; moreover, especially for BE30, they also found that NOx was measurably reduced [33,34].

Furthermore, the role of hydroxyl groups in n-butane and n-pentane has been shown to increase the reactivity of fuel molecules, accelerating the reaction rate and flame propagation in the combustion chamber, in which due to the bent of the carbon chain [35]. Unfortunately, from the background above, nothing has been revealed about the effect of using a mixture of bioethanol and isooctane on a stationary SI engine. Moreover, scientific information about the role of hydroxyl groups of bioethanol (see Fig. 1) in SI engines has not been identified until now. Therefore, this study aims to reveal new scientific information about the role of molecular properties and the performance of the BE50-isooctane fuel mixture on the stationary performance of the SI engine. In addition, a new approach was carried out by determining the optimal ignition timing range of 9°, 12°, and 15° BTDC.

2. Material and methods

The present research uses two samples of fuels; the first sample is 100% isooctane fuel, and the second is blended isooctane and bioethanol with a ratio v/v of 50%. Table 1 shows the physical and chemical properties of the fuels. Furthermore, to revealing the atomic and molecular properties (atomic properties, bond properties, and angle properties) of ethanol and isooctane, calculations were carried out using the molecular dynamics software, Avogadro version 1.2.0. The simulation results are shown in Tables 2–7.

The research scheme is shown in Fig. 2, and the outline of the test is as follows; The SI engine is run with a load obtained from the flow of water and is measured using a water brake dynamometer until the engine speed reaches a stable condition. The test engine used is a 125 cc SI engine and starts at 9° where the machine is in average condition, 12°, and 15° BTDC ignition timings. The engine runs from 3500 rpm to 7500 rpm and is carried out by cooling from the fan to minimize excess heat. Furthermore, every time the engine speed (rpm) changes, all engine performance parameters, engine temperature (°C), and engine pollutants are monitored, namely CO (%) and HC (ppm).

3. Fuels investigated

3.1. The molecular properties of ethanol and isooctane

Tables 2–7 show the results of investigations on the properties of the atoms and molecules that make up ethanol and isooctane compounds. The simulation results show that ethanol and isooctane are fuels that have unique properties and are composed of many components. This indicates that the combustion reaction that occurs is very complex and unique. Even for multi-component fuels, their molecular interactions and dynamics are phenomena that are difficult to understand until now [39]. Molecular dynamics analysis of the role and impact of the unique properties of ethanol and isooctane is described comprehensively in Section 3.2.

3.2. Molecular interaction of ethanol and isooctane

Based on previous research, it is known that the quantum chemical reaction of fuel in an internal combustion engine is complex [40], as it includes molecular modeling to determine the complexity of the combustion reaction of each active group, such as the hydroxyl group, the ethyl group, and the isooctane group [41]. On the other hand, from the bond properties data for ethanol (see Table 2) and isooctane (see Table 5), of the 9 bonds owned by ethanol, 8 bonds are non-rotatable, while isooctane has 23 non-rotatable bonds out of 25 bonds. This suggests that the majority of the molecular bonds of ethanol and isooctane have high and stable levels of rigidity, indicating that the carbon chain or other compounds besides it cannot affect the active group. Therefore, to describe the molecular interactions of ethanol, thus the carbon chain of ethanol is divided into two small molecular parts: the hydroxyl group and the ethyl group.

Table 1
The main properties of isooctane and ethanol.

Properties	Isooctane	Ethanol
Chemical formula	C_8H_{18}	C_2H_5OH
Purity (%)	99.5	99.7
Molecular weight ($g.mol^{-1}$)	114.23	46.07
Research octane number (RON) [36]	95.5	120–135
Auto-ignition temperature (^oC)	257 [37]	423
Specific heat (kJ/kg K)	2.4	2.0
Density at 20 °C ($g.cm^{-3}$)	691.9	789
Viskosity at 20 °C (mPa)	1.19 [32]	0.37–0.44
Stoichiometric A/F Ratio [8,38]	14.5	7.65

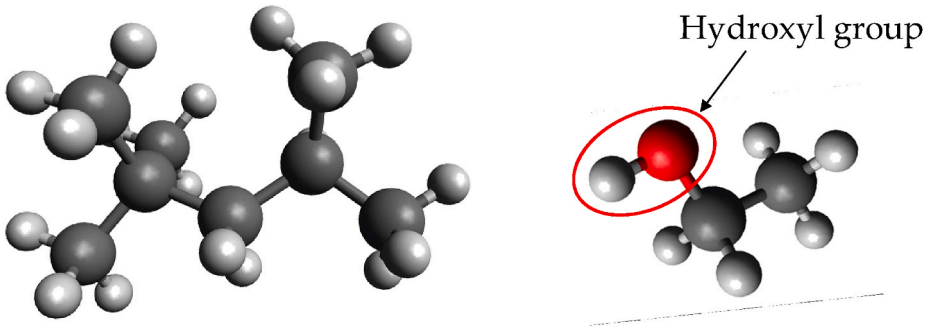

Fig. 1. The molecular structure of isooctane (left) and ethanol (right).

Table 2
Bond properties of Ethanol.

Bond	Type	Start atom	End atom	Rotatable
Bond 1	C–C	C1	C1	No
Bond 2	C–O	C2	O	No
Bond 3	O–H	O	H1	No
Bond 4	C–H	C1	H2	No
Bond 5	C–H	C1	H3	No
Bond 6	C–H	C1	H4	No
Bond 7	C–H	C2	H5	No
Bond 8	C–H	C2	H6	No

Table 3
Atom properties of Ethanol.

Atom	Element	Type	Valence	Formal charge	Partial charge
Atom 1	C	C3	4	0	−0.042
Atom 2	C	C3	4	0	0.041
Atom 3	O	O3	2	0	−0.395
Atom 4	H	HO	1	0	0.209
Atom 5	H	H	1	0	0.025
Atom 6	H	H	1	0	0.025
Atom 7	H	H	1	0	0.025
Atom 8	H	H	1	0	0.055
Atom 9	H	H	1	0	0.055

Table 4
Angle properties of Ethanol.

Angle	Type	Start atom	Vertex	End atom	Angle (°)
Angle 1	CCH	C2	C1	H2	109.7559
Angle 2	CCH	C2	C1	H3	110.0476
Angle 3	HCH	C2	C1	H4	110.0476
Angle 4	HCH	H2	C1	H3	108.9173
Angle 5	HCH	H2	C1	H4	108.9173
Angle 6	CCO	H3	C1	H4	109.1282
Angle 7	CCH	C1	C2	O	109.4386
Angle 8	CCH	C1	C2	H5	108.7301
Angle 9	OCH	C1	C2	H6	108.7304
Angle 10	OCH	O	C2	H5	109.9342
Angle 11	OCH	O	C2	H6	109.9341
Angle 12	HCH	H5	C2	H6	110.0453
Angle 13	COH	C2	O	H1	106.0429

Table 5
Bond properties of isooctane.

Bond	Type	Start atom	End atom	Rotatable
Bond 1	C–C	C1	C2	No
Bond 2	C–C	C1	C3	No
Bond 3	C–C	C1	C4	Yes
Bond 4	C–C	C1	C5	No
Bond 5	C–C	C4	C6	Yes
Bond 6	C–C	C6	C7	No
Bond 7	C–C	C6	C8	No
Bond 8	C–H	C2	H1	No
Bond 9	C–H	C2	H2	No
Bond 10	C–H	C2	H3	No
Bond 11	C–H	C3	H4	No
Bond 12	C–H	C3	H5	No
Bond 13	C–H	C3	H6	No
Bond 14	C–H	C5	H7	No
Bond 15	C–H	C5	H8	No
Bond 16	C–H	C5	H9	No
Bond 17	C–H	C6	H10	No
Bond 18	C–H	C4	H11	No
Bond 19	C–H	C4	H12	No
Bond 20	C–H	C7	H13	No
Bond 21	O–H	C7	H14	No
Bond 22	C–H	C7	H15	No
Bond 23	C–H	C8	H16	No
Bond 24	C–H	C8	H17	No
Bond 25	C–H	C8	H18	No

Table 6
Atom properties of isooctane.

Atom	Element	Type	Valence	Formal charge	Partial charge
Atom 1	C	C3	4	0	−0.037
Atom 2	C	C3	4	0	−0.060
Atom 3	C	C3	4	0	−0.060
Atom 4	C	C3	4	0	−0.046
Atom 5	C	C3	4	0	−0.060
Atom 6	C	C3	4	0	−0.046
Atom 7	C	C3	4	0	−0.063
Atom 8	C	C3	4	0	−0.063
Atom 9	H	H	1	0	0.023
Atom 10	H	H	1	0	0.023
Atom 11	H	H	1	0	0.023
Atom 12	H	H	1	0	0.023
Atom 13	H	H	1	0	0.023
Atom 14	H	H	1	0	0.023
Atom 15	H	H	1	0	0.023
Atom 16	H	H	1	0	0.023
Atom 17	H	H	1	0	0.023
Atom 18	H	H	1	0	0.030
Atom 19	H	H	1	0	0.027
Atom 20	H	H	1	0	0.027
Atom 21	H	H	1	0	0.023
Atom 22	H	H	1	0	0.023
Atom 23	H	H	1	0	0.023
Atom 24	H	H	1	0	0.023
Atom 25	H	H	1	0	0.023
Atom 26	H	H	1	0	0.023

Table 7
Angle properties of isooctane.

Angle	Type	Start atom	Vertex	End atom	Angle (°)
Angle 1	CCC	C2	C1	C3	108.5134
Angle 2	CCC	C2	C1	C4	110.8163
Angle 3	CCC	C2	C1	C5	109.7601
Angle 4	CCC	C2	C1	C4	107.4180
Angle 5	CCC	C3	C1	C5	106.7980
Angle 6	CCC	C4	C1	C5	113.3237
Angle 7	CCH	C1	C2	H1	110.6809
Angle 8	CCH	C1	C2	H2	110.7046
Angle 9	CCH	C1	C2	H3	110.8463
Angle 10	HCH	H1	C2	H2	108.2692
Angle 11	HCH	H1	C2	H3	108.6087
Angle 12	HCH	H2	C2	H3	107.6270
Angle 13	CCH	C1	C3	H4	111.0286
Angle 14	CCH	C1	C3	H5	110.7682
Angle 15	CCH	C1	C3	H6	111.0551
Angle 16	HCH	H4	C3	H5	108.1130
Angle 17	HCH	H4	C3	H6	107.6108
Angle 18	HCH	H5	C3	C6	108.7240
Angle 19	CCC	C1	C4	C6	121.1745
Angle 20	CCH	C1	C4	H11	105.5897
Angle 21	CCH	C1	C4	H12	108.7240
Angle 22	CCH	C1	C4	H11	104.4266
Angle 23	CCH	C6	C4	H12	109.1673
Angle 24	HCH	H11	C4	H12	106.7929
Angle 25	CCH	C1	C5	H7	110.6406
Angle 26	CCH	C1	C5	H8	110.1513
Angle 27	CCH	C1	C5	H9	113.8056
Angle 28	HCH	H7	C5	H8	107.9756
Angle 29	HCH	H7	C5	H9	108.8339
Angle 30	HCH	H8	C5	H9	105.1513
Angle 31	CCC	C4	C6	C7	108.4790
Angle 32	CCC	C4	C6	C8	115.0749
Angle 33	CCH	C4	C6	H10	109.5575
Angle 34	CCC	C7	C6	C8	108.2292
Angle 35	CCH	C7	C6	H10	106.7417
Angle 36	CCH	C8	C6	H10	108.4369
Angle 37	CCH	C6	C7	H13	110.5381
Angle 38	CCH	C6	C7	H14	110.8142
Angle 39	CCH	C6	C7	H15	110.5200
Angle 40	HCH	H13	C7	H14	108.7098
Angle 41	HCH	H13	C7	H15	107.4800
Angle 42	HCH	H14	C7	H15	108.6860
Angle 43	CCH	C6	C8	H16	110.9423
Angle 44	CCH	C6	C8	H17	111.7728
Angle 45	CCH	C6	C8	H18	109.9196
Angle 46	HCH	H16	C8	H17	110.7522
Angle 47	HCH	H16	C8	H18	108.5728
Angle 48	HCH	H17	C8	H18	104.6542

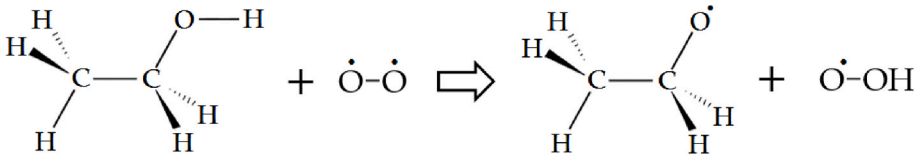

(1)

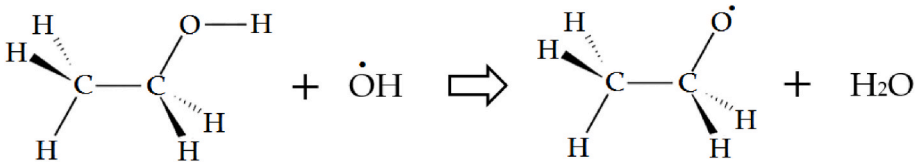

(2)

Reactions (1) and (2) illustrate the molecular dynamics of the OH group. When the OH group is attached to the C atom next to it, ethyl alcohol is established. It is also seen that the H atom in the O–H group changes its role to become the active center so that the oxidation reaction is easily achieved [42]; whereas, the OH group becomes a free radical for the oxygen-containing radical, OOH, and the free radical of H2O [18,43]. The results of this reaction indicate that the presence of the OH group has the potential to accelerate

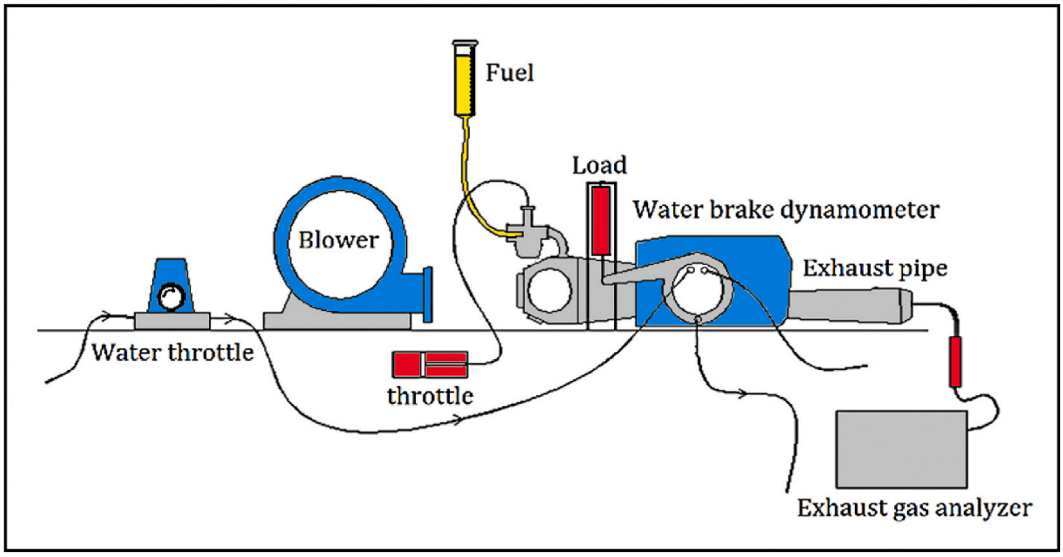

Fig. 2. The research apparatus.

the combustion process because the fuel molecules become reactive and easily react with oxygen. The presence of H_2O indicates that the OH molecule has the potential to be a coolant in the combustion chamber and produces environmentally friendly exhaust emissions. This is very reasonable because ethanol is a highly oxygenated fuel, has a high laminar flame propagation speed [44], and is a suitable coolant [45].

However, although the bonding properties of ethanol and iso-octane tend to be stable because they are composed of non-rotatable bonds, their atomic properties show another unique potential: ethanol has the largest partial charge, around δ^+ 0.20 and δ^- 0.39 (see Table 3), while isooctane is δ^+ 0.030 and δ^- 0.063 (see Table 6). These phenomena indicate that ethanol compounds have high reactivity; moreover, the large partial charge number indicates that there is an asymmetric distribution of electrons in each atomic bond, and consequently it makes ethanol polar, while isooctane is nonpolar [46,47].

Furthermore, Table 1 shows that the molecular weight of ethanol is 46.07 gmol-1, much smaller than isooctane, which is 114.23 g mol-1. The result indicates that the reactivity of the molecules is directly proportional to the increase in temperature and pressure in the combustion chamber, ethanol will be very reactive; when accompanied by a partial charge greater than isooctane, ethanol has the potential to induce isooctane. Consequently, there is an attractive force between the fuel molecules, thereby weakening the bonds between the carbon chains and decreasing the viscosity [26] so that the fuel is flammable [48]. This analysis is conceivable because when viewed from the angle properties of the ethanol compounds (see Table 4) and isooctane (see Table 7), the largest bond angle of isooctane is around 121.1745°, and the smallest is around 104.4266°. As for ethanol, the largest bond angle is 110.0476°, and the smallest was around 106.0429°. The difference in the degree of the bond angle and partial charge between ethanol and isooctane indicates that the molecular interactions between the fuel molecules of these two compounds have the potential to occur [35]. This can increase the reactivity of the fuel molecules so that it has the potential to improve the performance of the SI engine. This analysis is confirmed from the engine test data for all engine performance parameters (see Figs. 3–9).

4. Result and discussion

The molecular properties effect and the role of the OH group in the isooctane-BE50 fuel mixture and variations in ignition timing on the SI engine have been studied. The results showed that interesting phenomena occurred in all parameters of SI engine performance i. e. engine power, torque, thermal efficiency (ηth), sfc, energy consumption (EC), and the characteristics of exhaust gas emissions (CO and HC) produced.

Fig. 3 shows that with BE50, there is a decrease in torque due to the higher bioethanol content in isooctane [49] and the low specific thermal energy contained in the BE50 (see Table 1). Moreover, the phenomenon shows that the power increases, thus proving that with the difference in partial charge and the distance between the bond angles, the reactivity of the fuel molecules increases. On the other hand, Fig. 4 shows that when compared to isooctane, the engine power decreases. These results indicate that the presence of 8 molecular bonds of ethanol and 23 molecular bonds of non-rotatable isooctane has a great influence on the performance achieved. Moreover, this result also shows that at 12° ignition timing, the crankshaft angular speed angle becomes longer and increases the mass flow rate, and causes the engine load to increase, and this is confirmed by the high torque. Moreover, the result shows that the lowest power achieved by the BE50 engine occurs at low rpm, which is around 4000 rpm at 3.20 hp. At the same engine speed, the power produced by isooctane fuel is around 3.70 hp. While at high rpm around 6000 rpm–6500 rpm, the BE50-fueled engine reaches the highest power. This phenomenon indicates that at 6000 rpm–6500 rpm, the polarity of the OH group supported by the difference in partial charge and the large bond angle plays an important role in generating molecular interactions between the fuel molecules,

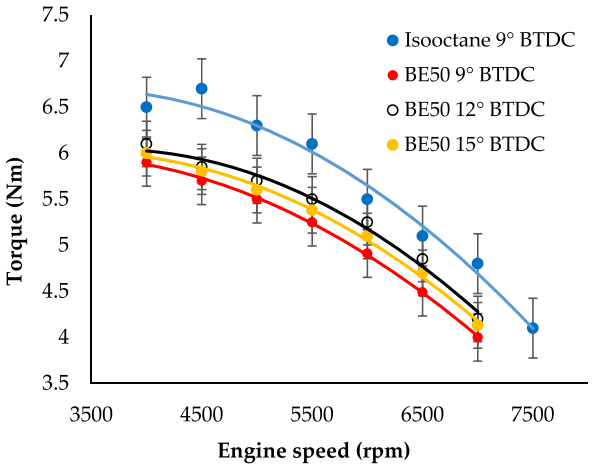

Fig. 3. Engine torque at various ignition timings.

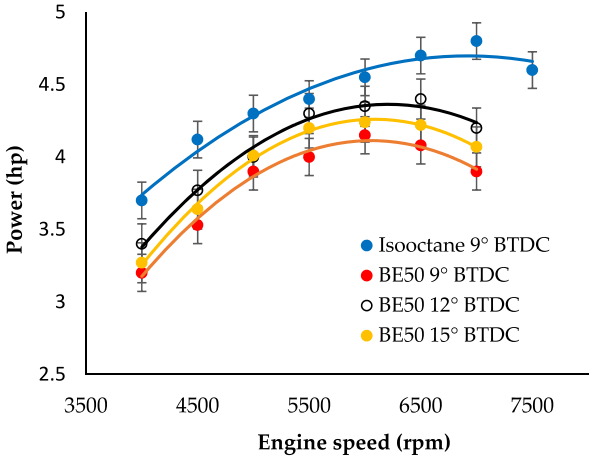

Fig. 4. Engine power at various ignition timings.

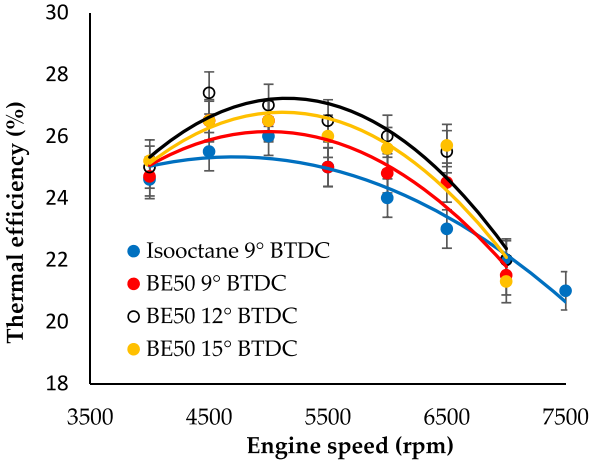

Fig. 5. Thermal efficiency of SI engine at various ignition timings.

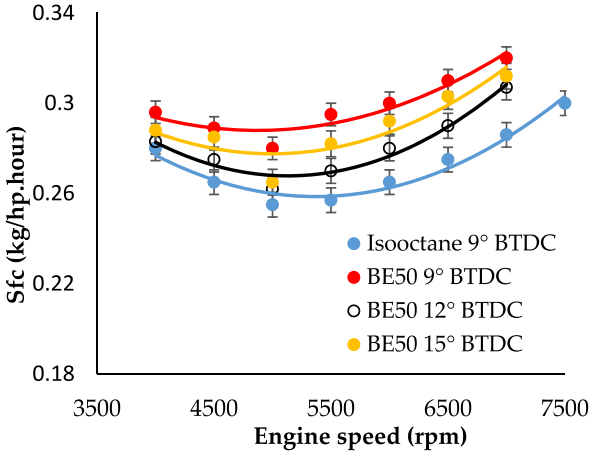

Fig. 6. Sfc of bioethanol and isooctane at various ignition timings.

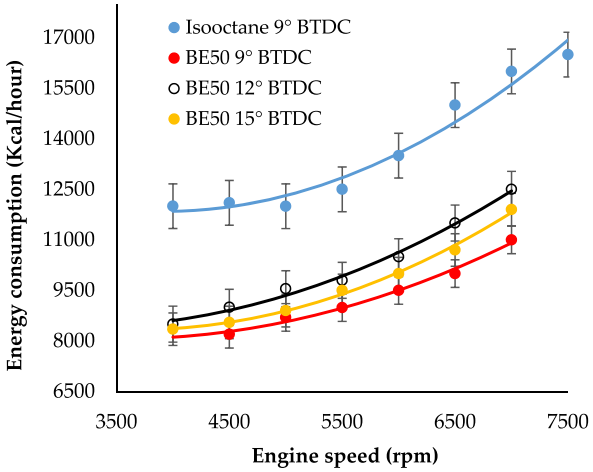

Fig. 7. Energy consumption of SI engine at various ignition timings.

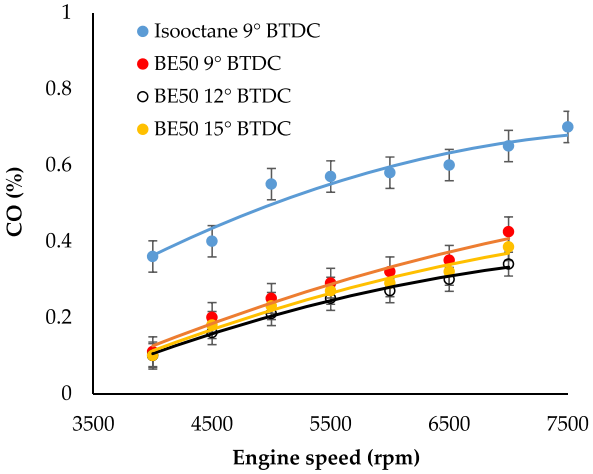

Fig. 8. CO emission of SI engine at various ignition timings.

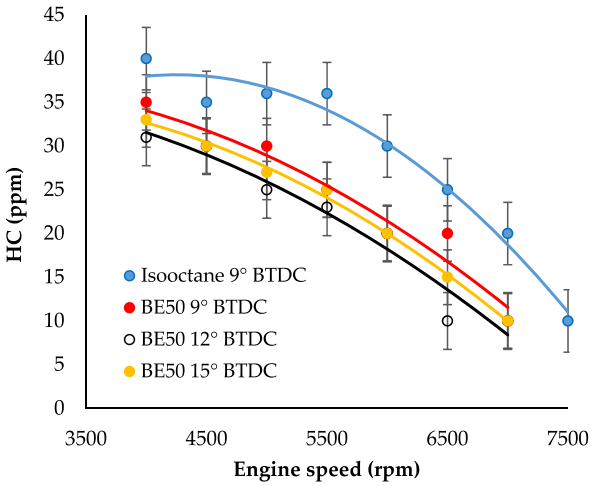

Fig. 9. HC emission of SI engine at various ignition timings.

thereby weakening the van der Waals binding force. This engine increase produces more power due to the reactivity of the fuel molecules. This analysis is consistent with previous studies, that the position of the OH group and its molecular geometry structure have an important role in decreasing viscosity so the burning rate increases [50].

Moreover, these results also indicate that at low speeds, the combustion temperature increases slowly because the active groups such as the hydroxyl group, ethyl group, and isooctane group also influence the exothermic rate. The molecular interactions of these three active groups cause the fuel molecules to take longer to react and burn. The majority of atomic bonds are non-rotatable (31 bonds; 8 ethanol and 23 isooctane); thus, they have a significant effect when the engine is at low speed, where spontaneous combustion occurs more slowly due to decreased liquid penetration [51] and combustion temperature, which reduces the exothermic rate [52].

Meanwhile, Fig. 5 shows that when the ignition timing is at 12°, the BE50-fueled engine produces the highest thermal efficiency. On the other hand, the lowest thermal efficiency of isooctane fuel occurs at 9°. These results indicate that the mass of the fuel decreases during the compression process and ignition. Whereas for isooctane, the decrease in fuel mass and increase in thermal efficiency is directly proportional to sfc, where fuel consumption becomes more efficient when this occurs at 9°. This phenomenon indicates that changes in thermal efficiency are affected by the high reactivity of fuel molecules [53].

Furthermore, these results also show that the ignition time of 12° is the time at which the molecules of the fuel mixture of isooctane and BE50 become more reactive than the other conditions. This phenomenon also indicates that the geometry of bioethanol in the form of a branched chain and the polarity of the hydroxyl group make the fuel more polar. The analysis is consistent with previous studies using n-butanol and n-pentanol, they stated that although n-butanol and n-pentanol have a straight chain, the presence of the OH molecule can increase the interaction between droplets [48] thereby accelerating the flame speed and flame propagation in the combustion chamber [54]. Moreover, this is also supported by the large difference in the partial charge between ethanol and isooctane, namely δ^+ 0.209 and δ^- 0.395 for ethanol, while isooctane is δ^+ 0.030 and δ^- 0.063 (see Tables 3 and 6). Due to the difference in partial charge, the attraction and repulsion between the two compounds increases, which results in a corresponding increase in the reactivity of the fuel molecules.

Fig. 7 shows the impact of changes in ignition timing on energy consumption. Isooctane has the highest level of energy consumption, which is around 16,500 kcal/h at 7500 RPM, while for BE50; the highest energy consumption is achieved at 12° ignition timing of around 12,000 kcal/h at 7000 RPM. This indicates that the use of BE50 results in energy consumption savings of around 25.44%. Molecularly, this phenomenon suggests that the presence of the OH group is influential in producing fuel with high thermal efficiency and less energy consumption. This analysis is plausible the presence of a polar and branched OH group indicates that the molecules of BE50 more reactive, a finding that is confirmed by the higher thermal efficiency compared to the isooctane. In addition, this phenomenon also indicates that a mixture of 50% bioethanol and 50% isooctane can increase the mass density of the fuel; as a result, an effective collision occurs due to the closer the distance between the fuel molecules. This analysis is committed to previous researcher, they stated that the isooctane-bioethanol mixture could reducing the potential for knocking due to the increase the intensity and interaction between the flame and the combustion pressure in the combustion chamber [10,55].

In addition, from Fig. 8, when compared with isooctane, BE50 has a reduction in carbon monoxide content of 58.97%, and this occurs at an ignition time of 12°. The same result is derived from hydrocarbon emissions, where the highest HC content occurred in isooctane fuel, and the lowest was achieved by BE50 when the ignition time was 12°. When compared with pure isooctane, it show that at the 12° BTDC there was a 36.29% reduction in HC gas emissions (see Fig. 9). The reduction in CO and HC gas emissions suggests that BE50 is an environmentally friendly fuel with low soot emissions [56] and is suitable for use as a renewable energy for SI engines [57].

5. Conclusion

A comprehensive study of the presence of the hydroxyl molecules and the effect of molecular properties and various ignition timings on the SI engine with isooctane-bioethanol has been carried out, and the significant scientific findings, as follows:

- The presence of OH groups and the bent geometry of the bioethanol carbon chain have a crucial role in increasing the polarity and reactivity of fuel molecules. Therefore, fuel performance improves, as evidenced by power and torque; moreover, good thermal efficiency can be produced with more efficient sfc and less energy consumption.
- The nature of the large partial charge in the atoms that make up the ethanol compound produces an asymmetric distribution of electrons in each atomic bond; thereby, the reactivity of the fuel molecules was increased. This becomes useful in reducing the negative impact of the bond properties of ethanol and isooctane, which tend to be non-rotatable or rigid.
- Differences in bond angles and partial charges of ethanol and isooctane compounds create molecular interactions with high reactivity between fuel molecules, thus resulting environmentally friendly combustion process as evidenced by lower CO and HC emissions.
- The optimal ignition timing for an isooctane-fueled SI engine is 9°, while for bioethanol it is 12° BTDC. In addition, the improved performance of the BE50 fuel engine proves that the BE50 can be relied upon as a renewable fuel by changing the ignition timing at 12° BTDC.
- The study of bioethanol can be continued, this is very important because previous studies stated that SI engines (normal conditions) with bioethanol produce different performances. Moreover, the complexity of the molecular dynamics between atoms and fuel molecules must be further explored to produce new scientific information, which is useful for the development of scientific research regarding fuel engineering and combustion technology.

Author contribution statement

Suyatno and Helen Riupassa: Conceived and designed the experiments; Performed the experiments; Analyzed and interpreted the data; Contributed reagents, materials, analysis tools or data; Wrote the paper. Susi Marianingsih: Analyzed and interpreted the data; Contributed reagents, materials, analysis tools or data; Wrote the paper. Hendry Y. Nanlohy: Performed the experiments; Analyzed and interpreted the data; Wrote the paper.

Funding statement

Dr. Hendry Y. Nanlohy was supported by Kementrian Pendidikan, Kebudayaan, Riset, Dan Teknologi Republik Indonesia [1058/LL14/PG.02.00.PT/2022].

Data availability statement

Data included in article/supp. material/referenced in article.

Declaration of competing interest

The authors declare no conflict of interest.

Acknowledgement

Thanks to the Fuel and Combustion Laboratory of the Department of Mechanical Engineering, Jayapura University of Science and Technology, for the support of research materials and equipment. Thanks also to Prof. Toshihisa Ueda, Ph.D and Prof. ING Wardana. Ph.D for the critical review, and especially for the valuable perspective on the role of fuel molecular.

References

[1] S.M. Safieddin Ardebili, H. Solmaz, D. İpci, A. Calam, M. Mostafaei, A review on higher alcohol of fusel oil as a renewable fuel for internal combustion engines: applications, challenges, and global potential, Fuel 279 (2020), https://doi.org/10.1016/j.fuel.2020.118516. April.
[2] B. Sayin Kul, M. Ciniviz, An evaluation based on energy and exergy analyses in SI engine fueled with waste bread bioethanol-gasoline blends, Fuel 286 (P2) (2021) 119375, https://doi.org/10.1016/j.fuel.2020.119375.
[3] S. Chen, A. Kharrazi, S. Liang, B.D. Fath, M. Lenzen, J. Yan, Advanced approaches and applications of energy footprints toward the promotion of global sustainability, Appl. Energy 261 (2020) 114415, https://doi.org/10.1016/J.APENERGY.2019.114415. Mar.
[4] K. Salelign, R. Duraisamy, Sugar and ethanol production potential of sweet potato (Ipomoea batatas) as an alternative energy feedstock: processing and physicochemical characterizations, Heliyon 7 (11) (2021), e08402, https://doi.org/10.1016/j.heliyon.2021.e08402.
[5] A. Elfasakhany, Gasoline engine fueled with bioethanol-bio-acetone-gasoline blends: performance and emissions exploration, Fuel 274 (2020) 117825, https://doi.org/10.1016/j.fuel.2020.117825. April.
[6] M. Mukherjee, G. Goswami, P.K. Mondal, D. Das, Biobutanol as a potential alternative to petroleum fuel: sustainable bioprocess and cost analysis, Fuel 278 (2020), 118403, https://doi.org/10.1016/j.fuel.2020.118403. May.

[7] S. Di Iorio, F. Catapano, A. Magno, P. Sementa, B.M. Vaglieco, Investigation on sub-23 nm particles and their volatile organic fraction (VOF) in PFI/DI spark ignition engine fueled with gasoline, ethanol and a 30 %v/v ethanol blend, J. Aerosol Sci. 153 (2021) 105723, https://doi.org/10.1016/j.jaerosci.2020.105723. July.

[8] M. Göktaş, M. Kemal Balki, C. Sayin, M. Canakci, An evaluation of the use of alcohol fuels in SI engines in terms of performance, emission and combustion characteristics: a review, Fuel 286 (2021), https://doi.org/10.1016/j.fuel.2020.119425. July 2020.

[9] P.S. Awodi, J.C. Ogbonna, T.N. Nwagu, Bioconversion of mango (Mangifera indica) seed kernel starch into bioethanol using various fermentation techniques, Heliyon 8 (6) (2022), e09707, https://doi.org/10.1016/j.heliyon.2022.e09707.

[10] J. Wei, H. Feng, H. Liu, H. Zhu, Z. Yue, M. Yao, Analysis of knocking combustion with methanol/iso-octane and ethanol/iso- octane blends in a spark-ignition engine, Fuel 284 (2021) 118979, https://doi.org/10.1016/j.fuel.2020.118979. August 2020.

[11] M. Nibin, J.B. Raj, V.E. Geo, Experimental studies to improve the performance, emission and combustion characteristics of wheat germ oil fuelled CI engine using bioethanol injection in PCCI mode, Fuel 285 (2021) 119196, https://doi.org/10.1016/j.fuel.2020.119196. April 2020.

[12] H.Y. Nanlohy, H. Riupassa, An Experimental Study on the Ignition Behavior of Blended Fuels Droplets with Crude Coconut Oil and Liquid Metal Catalyst, vol. 3, 2020, pp. 39–45, no. 2.

[13] D.Y. Dhande, N. Sinaga, K.B. Dahe, Study on combustion, performance and exhaust emissions of bioethanol-gasoline blended spark ignition engine, Heliyon 7 (3) (2021), e06380, https://doi.org/10.1016/j.heliyon.2021.e06380.

[14] A.S. Auzani, A.G. Clements, K.J. Hughes, D.B. Ingham, M. Pourkashanian, Assessment of ethanol autoxidation as a drop-in kerosene and surrogates blend with a new modelling approach, Heliyon 7 (6) (2021), e07295, https://doi.org/10.1016/j.heliyon.2021.e07295.

[15] V.L. Dagle, M. Affandy, Lopez, Production, fuel properties and combustion testing of an iso-olefins blendstock for modern vehicles, Fuel 310 (2022) 122314, https://doi.org/10.1016/J.FUEL.2021.122314. Feb.

[16] F. Catapano, S. Di Iorio, A. Magno, B.M. Vaglieco, Effect of fuel quality on combustion evolution and particle emissions from PFI and GDI engines fueled with gasoline, ethanol and blend, with focus on 10–23 nm particles, Energy 239 (2022) 122198, https://doi.org/10.1016/J.ENERGY.2021.122198. Jan.

[17] Q. Fan, Y. Qi, Y. Wang, Z. Wang, Investigation into pressure dependence of flame speed for fuels with low and high octane sensitivity through blending ethanol, Combust. Flame 212 (Feb. 2020) 252–269, https://doi.org/10.1016/J.COMBUSTFLAME.2019.10.040.

[18] N. Sekularac, X.H. Fang, V. Shankar, S.J. Baker, F.C.P. Leach, M.H. Davy, Development of a laminar burning velocity empirical correlation for combustion of iso-octane/ethanol blends in air, Fuel 307 (2022) 121880, https://doi.org/10.1016/j.fuel.2021.121880. September 2021.

[19] D. Firew, R.B. Nallamothu, G. Alemayehu, R. Gopal, Performance and emission evaluation of CI engine fueled with ethanol diesel emulsion usingNiZnFe2O4 nanoparticle additive, Heliyon 8 (2022), e11639, https://doi.org/10.1016/j.heliyon.2022.e11639. May.

[20] J. Badra, F. Alowaid, A. Alhussaini, A. Alnakhli, Understanding of the octane response of gasoline/MTBE blends, Fuel 318 (2022) 123647, https://doi.org/10.1016/j.fuel.2022.123647. November 2021.

[21] Q. Fan, Z. Wang, Y. Qi, S. Liu, X. Sun, Research on ethanol and toluene's synergistic effects on auto-ignition and pressure dependences of flame speed for gasoline surrogates, Combust. Flame 222 (Dec. 2020) 196–212, https://doi.org/10.1016/J.COMBUSTFLAME.2020.08.049.

[22] B. Wang, Y. Li, Y. Jiang, H. Xu, X. Zhang, Dynamic spray development of 2-methylfuran compared to ethanol and isooctane under ultra-high injection pressure, Fuel 234 (2018) 581–591, https://doi.org/10.1016/j.fuel.2018.06.013. July.

[23] J. Yan, S. Gao, W. Liu, T. Chen, T.H. Lee, C. Lee, Experimental study of flash boiling spray with isooctane , hexane , ethanol and their binary mixtures, Fuel 292 (2021) 120415, https://doi.org/10.1016/j.fuel.2021.120415. July 2020.

[24] T. Badawy, H. Xu, Y. Li, Macroscopic spray characteristics of iso -octane , ethanol , gasoline and methanol from a multi-hole injector under flash boiling conditions, Fuel 307 (2022) 121820, https://doi.org/10.1016/j.fuel.2021.121820. August 2021.

[25] Z. Guo, X. Yu, G. Li, Y. Sun, Z. Zhao, D. Li, Comparative study of different injection modes on combustion and particle emission of acetone-butanol-ethanol (ABE) and gasoline in a dual-injection SI engine, Fuel 281 (2020) 118786, https://doi.org/10.1016/j.fuel.2020.118786. June.

[26] H.Y. Nanlohy, Performance and emissions analysis of BE85-gasoline blends on spark ignition engine, Autom. Exp. 5 (1) (2022) 40–48, 10316/ae.6116.

[27] Y. Qian, Z. Li, L. Yu, X. Wang, X. Lu, Review of the state-of-the-art of particulate matter emissions from modern gasoline fueled engines, Appl. Energy 238 (2019) 1269–1298, https://doi.org/10.1016/J.APENERGY.2019.01.179. Mar.

[28] Y. Su, Y. Zhang, F. Xie, J. Duan, X. Li, Y. Liu, Influence of ethanol blending ratios on in-cylinder soot processes and particulate matter emissions in an optical direct injection spark ignition engine, Fuel 308 (2022) 121944, https://doi.org/10.1016/j.fuel.2021.121944. June 2021.

[29] H. Taghavifar, B.K. Kaleji, J. Kheyrollahi, Application of composite TNA nanoparticle with bio-ethanol blend on gasoline fueled SI engine at different lambda ratios, Fuel 277 (May) (2020) 118218, https://doi.org/10.1016/j.fuel.2020.118218.

[30] B. Sayin Kul, M. Ciniviz, Assessment of waste bread bioethanol-gasoline blends in respect to combustion analysis, engine performance and exhaust emissions of a SI engine, Fuel 277 (2020) 118237, https://doi.org/10.1016/j.fuel.2020.118237. April.

[31] P. Sakthivel, K.A. Subramanian, R. Mathai, Experimental study on unregulated emission characteristics of a two-wheeler with ethanol-gasoline blends (E0 to E50), Fuel 262 (2020) 116504, https://doi.org/10.1016/j.fuel.2019.116504. August 2019.

[32] H.Y. Nanlohy, H. Riupassa, M. Yamaguchi, Performance and emissions analysis of BE85-gasoline blends on spark ignition engine, Autom. Exp. 5 (1) (2022) 40–48, https://doi.org/10.31603/ae.6116.

[33] Z. Guo, X. Yu, Dong, Research on the combustion and emissions of an SI engine with acetone-butanol-ethanol (ABE) port injection plus gasoline direct injection, Fuel 267 (2020) 117311, https://doi.org/10.1016/j.fuel.2020.117311. February.

[34] Z. Liu, P. Sun, Y. Du, X. Yu, W. Dong, J. Zhou, Improvement of combustion and emission by combined combustion of ethanol premix and gasoline direct injection in SI engine, Fuel 292 (2021) 120403, https://doi.org/10.1016/j.fuel.2021.120403. November 2020.

[35] H.Y. Nanlohy, I.N.G. Wardana, M. Yamaguchi, T. Ueda, The role of rhodium sulfate on the bond angles of triglyceride molecules and their effect on the combustion characteristics of crude jatropha oil droplets, Fuel 279 (2020), https://doi.org/10.1016/j.fuel.2020.118373. February.

[36] A. da Silva, J. Hauber, L.R. Cancino, K. Huber, The research octane numbers of ethanol-containing gasoline surrogates, Fuel 243 (2019) 306–313, https://doi.org/10.1016/j.fuel.2019.01.068. November 2018.

[37] J. Li, J. Zhu, Wang, An experimental and modeling study of autoignition characteristics of two real low-octane gasoline fuels in a heated rapid compression machine at elevated pressures, Fuel 295 (2021) 120645, https://doi.org/10.1016/J.FUEL.2021.120645. Jul.

[38] H.Y. Nanlohy, H. Riupassa, T. Trismawati, M.S. Panithasan, Gasohol engine performance with various ignition timing, J. Mech. Eng. Sci. Technol. 6 (1) (2022) 48, https://doi.org/10.17977/um016v6i12022p048.

[39] S.S. Sazhin, Modelling of fuel droplet heating and evaporation: recent results and unsolved problems, Fuel 196 (2017) 69–101, https://doi.org/10.1016/j.fuel.2017.01.048.

[40] R. Oviedo-Roa, J.F. Ramírez-Pérez, Servín-Nájera, Quantum molecular modeling of oxazolidines as detergent-dispersant additives for gasoline: a valuable technological adviser, Fuel 315 (2022) 122715, https://doi.org/10.1016/J.FUEL.2021.122715. May.

[41] H. Zhu, Y. Huo, W. Wang, X. He, S. Fang, Y. Zhang, Quantum chemical calculation of reaction characteristics of hydroxyl at different positions during coal spontaneous combustion, Process Saf. Environ. Protect. 148 (2021) 624–635, https://doi.org/10.1016/j.psep.2020.11.041.

[42] H.Y. Nanlohy, Trismawati, The role of fatty acid of Morinda citrifolia oil as surface-active chemicals on the deinking process of waste paper, Materialia 23 (2022) 101436, https://doi.org/10.1016/J.MTLA.2022.101436. Jun.

[43] D. Jesu Godwin, V. Edwin Geo, Thiyagarajan, Effect of hydroxyl (OH) group position in alcohol on performance, emission and combustion characteristics of SI engine, Energy Convers. Manag. 189 (2019) 195–201, https://doi.org/10.1016/j.enconman.2019.03.063. March.

[44] M.K. Mohammed, H.H. Balla, Z.M.H. Al-Dulaimi, Z.S. Kareem, M.S. Al-Zuhairy, Effect of ethanol-gasoline blends on SI engine performance and emissions, Case Stud. Therm. Eng. 25 (2021) 100891, https://doi.org/10.1016/j.csite.2021.100891. May 2020.

[45] X. Duan, Y. Li, Y. Liu, J. Liu, S. Wang, G. Guo, Quantitative investigation the influences of the injection timing under single and double injection strategies on performance, combustion and emissions characteristics of a GDI SI engine fueled with gasoline/ethanol blend, Fuel 260 (2020) 116363, https://doi.org/10.1016/j.fuel.2019.116363. October 2019.

[46] Y. Duan, A. Zhong, Z. Huang, D. Han, Theoretical study on hydrogen abstraction reactions from cyclopentanol by hydroxyl radical, Fuel 297 (2021) 120766, https://doi.org/10.1016/j.fuel.2021.120766. March.
[47] C. Esonye, O.D. Onukwuli, V.C. Anadebe, J.N.O. Ezeugo, N.J. Ogbodo, Application of soft-computing techniques for statistical modeling and optimization of Dyacrodes edulis seed oil extraction using polar and non-polar solvents, Heliyon 7 (3) (2021), e06342, https://doi.org/10.1016/j.heliyon.2021.e06342.
[48] H.Y. Nanlohy, I.N.G. Wardana, N. Hamidi, L. Yuliati, T. Ueda, The effect of Rh3+ catalyst on the combustion characteristics of crude vegetable oil droplets, Fuel 220 (2018) 220–232, https://doi.org/10.1016/j.fuel.2018.02.001. December 2017.
[49] C.Y. Lee, X. Cheng, H. Mun Poon, S. Reddy Yelugoti, W.C. Wang, The spray ignition characteristics of ethanol blended with hydro-processed renewable diesel in a constant volume combustion chamber, Fuel 314 (2022) 123089, https://doi.org/10.1016/J.FUEL.2021.123089. Apr.
[50] B. Rotavera, C.A. Taatjes, Influence of functional groups on low-temperature combustion chemistry of biofuels, Prog. Energy Combust. Sci. 86 (xxxx) (2021), 100925, https://doi.org/10.1016/j.pecs.2021.100925.
[51] R. Kale, R. Banerjee, Understanding spray and atomization characteristics of butanol isomers and isooctane under engine like hot injector body conditions, Fuel 237 (2019) 191–201, https://doi.org/10.1016/J.FUEL.2018.09.142. Feb.
[52] B. Gainey, B. Lawler, The role of alcohol biofuels in advanced combustion: an analysis, Fuel 283 (2021) 118915, https://doi.org/10.1016/j.fuel.2020.118915. June 2020.
[53] O.I. Awad, R. Mamat, Ibrahim, Overview of the oxygenated fuels in spark ignition engine: environmental and performance, Renew. Sustain. Energy Rev. 91 (2018) 394–408, https://doi.org/10.1016/j.rser.2018.03.107. March.
[54] Y. Jiang, H. Xu, X. Ma, X. Bao, B. Wang, Laminar burning characteristics of 2-MTHF compared with ethanol and isooctane, Fuel 190 (2017) 10–20, https://doi.org/10.1016/j.fuel.2016.11.036.
[55] H. Shi, Q. Tang, K. Uddeen, B. Johansson, J. Turner, G. Magnotti, Effects of multiple spark ignition on engine knock under different compression ratio and fuel octane number conditions, Fuel 310 (2022) 122471, https://doi.org/10.1016/J.FUEL.2021.122471. Feb.
[56] H. Aljabri, X. Liu, Al-lehaibi, Fuel flexibility potential for isobaric combustion in a compression ignition engine: a computational study, Fuel 316 (May 2022) 123281, https://doi.org/10.1016/J.FUEL.2022.123281.
[57] X. Yu, Z. Zhao, Huang, Experimental study on the effects of EGR on combustion and emission of an SI engine with gasoline port injection plus ethanol direct injection, Fuel 305 (2021) 121421, https://doi.org/10.1016/j.fuel.2021.121421. August.